J som spänningsintensitetsparameter

För icke-linjära mtrl: HRR- Hutchinson Rice Rosengren singularitet.

Ramberg-Osgood:

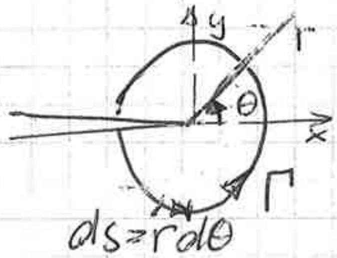

$$\varepsilon = \frac{\sigma}{E} + \left(\frac{\sigma}{A'}\right)^{1/n'} = \frac{\sigma}{E} + \left(\frac{\sigma}{A'}\right)^{n}$$

$$J = \int_\Gamma \left(W\,dy - \sigma_{ij} n_j \frac{\partial u_i}{\partial x} ds\right) \qquad W = \int^{\varepsilon_{ij}} \sigma_{ij}\, d\varepsilon_{ij}$$

I plastiska zonen:

$$\varepsilon \sim \sigma^n \quad d\varepsilon \sim \sigma^{n-1} d\sigma$$

$$W \sim \int \sigma \sigma^{n-1} d\sigma = \int \sigma^n d\sigma = \frac{\sigma^{n+1}}{n+1} \sim \sigma \sigma^n \sim \sigma \varepsilon$$

Väg Γ runt spetsen: $ds = r\,d\theta$

J: $J \sim \int_\Gamma \sigma \varepsilon\, ds = \int_\Gamma \underbrace{\sigma \varepsilon}\, r\, d\theta$

$\sigma\varepsilon \sim \frac{1}{r}$ om J ändlig då $r \to 0$

Sätt $\varepsilon \sim r^\lambda$; $\varepsilon\sigma \sim \frac{1}{r} \Rightarrow \sigma \sim r^{-(1+\lambda)}$

Ramberg-Osgood: $\varepsilon \sim \sigma^n$; $r^\lambda \sim r^{-n(1+\lambda)} \Rightarrow \lambda = -\frac{n}{1+n}$

Alltså: $\varepsilon \sim r^{-\frac{n}{1+n}}$ $\quad \sigma \sim r^{-\frac{1}{n+1}}$

HRR-singulära fält:

n=1: Linjärt elastiskt

$$\begin{cases} \sigma_{ij} = \sigma_Y \left(\dfrac{J}{\alpha \sigma_Y \varepsilon_Y I_n r}\right)^{\frac{1}{n+1}} \tilde{\sigma}_{ij}(\theta, n) \qquad I_n = I_n(n) \\ \varepsilon_{ij} = \alpha \varepsilon_Y \left(\dfrac{J}{\alpha \sigma_Y \varepsilon_Y I_n r}\right)^{\frac{n}{n+1}} \tilde{\varepsilon}_{ij}(\theta, n) \\ u_i = \alpha \varepsilon_Y \left(\dfrac{J}{\alpha \sigma_Y \varepsilon_Y I_n}\right)^{\frac{n}{n+1}} r^{\frac{1}{n+1}} \tilde{u}_i(\theta, n) \end{cases}$$

J definierar alltså amplituden i HRR-fältet

K vid LEFM

9.7 J-dominans

I plastiska zonen: HRR-singularitet $\sigma_{ij} \sim \left(\frac{J}{r}\right)^{\frac{1}{n+1}}$, $\varepsilon_{ij} \sim \left(\frac{J}{r}\right)^{\frac{n}{n+1}}$

Elastiskt: $n=1$, $\sigma_{ij} \sim \frac{1}{\sqrt{r}}$, $\varepsilon_{ij} \sim \frac{1}{\sqrt{r}}$

Båda ger ∞ sp. töjn. då $r \to 0$. I verkligheten blir

SSY: K och J

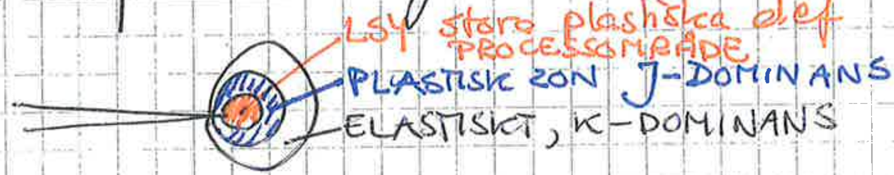

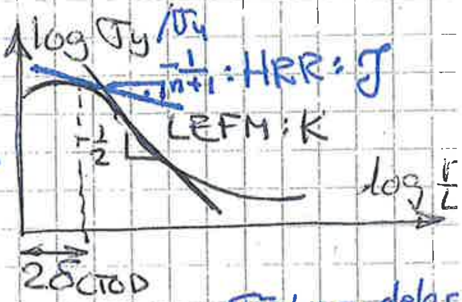

ELASTISK-PLASTISK: J och CTOD

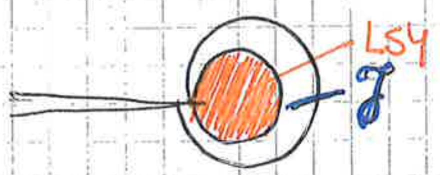

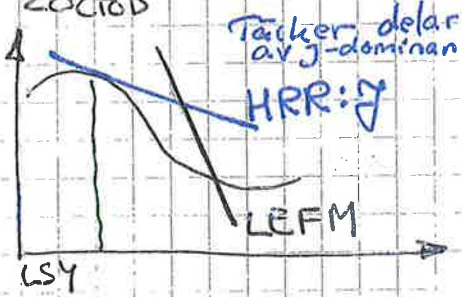

LARGE SCALE YIELDING

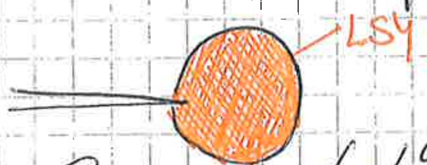

Enparameterlösningar gäller ej

9.8 TVÅPARAMETERFRAMSTÄLLNINGAR

SSY, elastiska lösningar: $\boxed{\text{T-stress}}$ ← 2 termer i Williams expansion

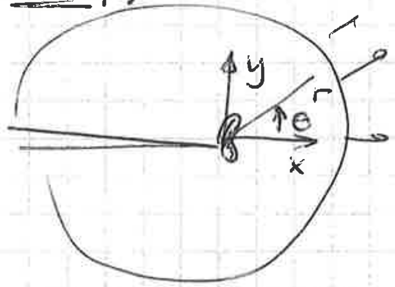

$$\sigma_{ij} = \frac{K_I}{\sqrt{2\pi r}} f_{ij}(\theta) + T\delta_{1i}\delta_{1j} = \frac{K_I}{\sqrt{2\pi r}} f_{ij} + \begin{bmatrix} T & 0 & 0 \\ 0 & 0 & 0 \\ 0 & 0 & +\nu T \end{bmatrix}$$ plan töj.

T förblir ändlig då $r \to 0$

T påverkar sp i plast zonen

zonens storlek

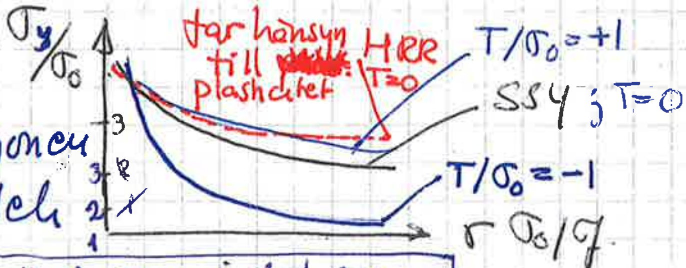

$\boxed{\text{J–Q–THEORY}}$: LSY

Djupt inne i plast zonen: $\sigma_{ij} = \sigma_{ij\,HRR} + \sigma_{ij\,diff}$ MÄTER TRIAXIALITETEN VID SPRICKSPETSEN

Alt Inne i plastiska zonen: $\sigma_{ij} \approx (\sigma_{ij})_{T=0} + Q\sigma_y\delta_{ij}$ $\quad |\theta| \le \frac{\pi}{2}$

$\frac{J}{\sigma_y} < r < \frac{5J}{\sigma_y}$ DEF: $\quad Q = \dfrac{\sigma_{\theta\theta} - (\sigma_{\theta\theta})_{HRR}}{\sigma_y} \quad \theta = 0 \quad r = \dfrac{2J}{\sigma_y}$

ELLER $\quad Q = \dfrac{\sigma_{\theta\theta} - (\sigma_{\theta\theta})_{SSY,T=0}}{\sigma_y} \quad \theta = 0 \quad r = \dfrac{2J}{\sigma_y}$

ELLER $\quad Q = \dfrac{\sigma_m - (\sigma_m)_{SSY,T=0}}{\sigma_y} \quad \theta = 0 \quad r = \dfrac{2J}{\sigma_y}$

POS Q ÖKAR ÖKAR HYDR. SP. JFRT MED HRR-FÄLTET ELLER SSY-LÖSNINGEN

Q MINSKA → MINSKNING

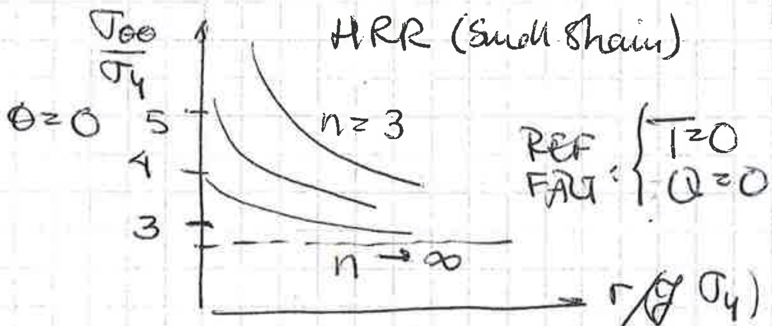

REF FÄLT: T=0, Q=0

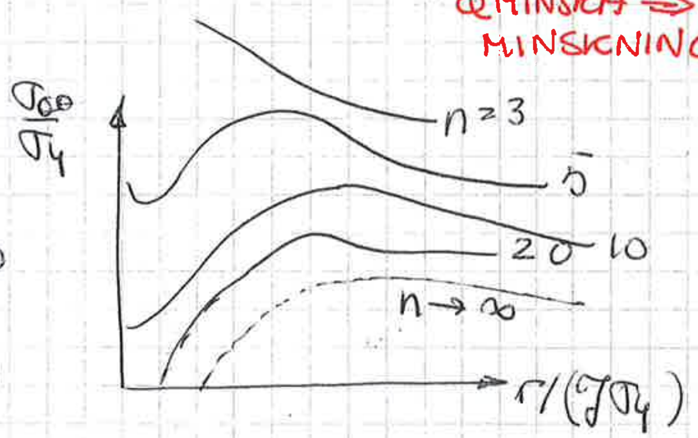

$$\sigma_{ij} = \sigma_y \left(\frac{J}{\alpha\sigma_y\varepsilon_y I_n r}\right)^{\frac{1}{n+1}} \tilde{\sigma}_{ij}(\theta, n)$$

Fig 9.13

Q bäst utanför $\underbrace{\text{trubbningszonen}}_{\text{med ändliga töjn.}}$ ⇒ Q ober av r

X

4.2 Fretting maps

To characterize how a specific material responds to fretting and in order to classify experimental data, fretting maps are used. The concept of fretting maps was introduced by Vingsbo and Söderberg [5] in 1986. Fretting maps illustrate the events in-between two moving surfaces in contact in a diagram of two variables. Several parameters can be monitored to create the fretting map, e.g. normal force, friction force or slip amplitude. To create a fretting map, two independently varying parameters are chosen whereas all other parameters are kept constant. The accuracy of the fretting map depends on the accuracy of included parameters and on the actual constancy of all parameters, not pictured in the fretting map. Despite this, fretting maps are useful and informative in characterizing fretting conditions, including damage.

Two types of fretting maps have been proposed by Jin and Mall [9]; the material response fretting map (MRFM), illustrating the material response for different load cases, and the running condition fretting map (RCFM), describing the state of contact between the two surfaces. In Figure 7 a RCFM in combination with a MRFM is shown [10].

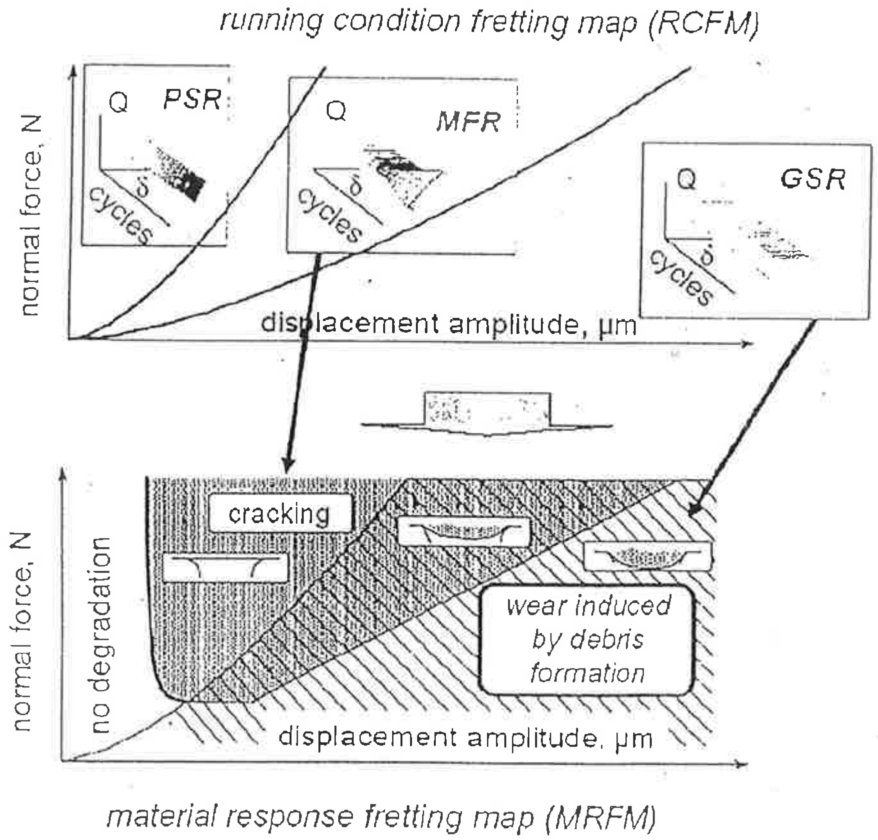

Figure 7. A combination of a RCFM with a MRFM. The RCFM involves the partial slip regime (PSR), the mixed fretting regime (MFR) and the gross slip regime (GSR) [10].

( ) : numerics, cast iron, welds } we have not done

Loadings

fe-safe™ can predict fatigue lives from a range of loading types:

- Single load time history applied to a linear elastic finite element model
- Multiple time histories of loading superimposed in fe-safe™ (more than 4000 load histories can be applied) Palmgren-Miner
- Sequence of FEA stresses (elastic or elastic-plastic, linear or non-linear) Hooke Ramberg-Osgood
- ( ) Superimposition of steady state modal solutions
- ( ) Superimposition of transient dynamic modal solutions NO
- PSD loading, block loading test programmes, rainflow cycle matrices
- ( ) Effects of forming or assembly stresses can be included

Palmgren-Miner

Fatigue contour plot of a bracket

fe-safe™ includes a powerful simple-to-use batch command system, with on-line parametric variation for 'sensitivity' studies.

Standard analyses can be set up and saved for re-use.

Analysis methods

ALL TOTAL LIFE METHODS. NO FRACTURE MECHANICS

fe-safe™ includes an extensive range of analysis methods, all of which are included in the standard package:

- Strain-based multiaxial fatigue algorithms – axial strain, shear strain, Brown-Miller from FEA stresses, with a multiaxial Neuber's rule and cyclic plasticity model Morrow Ramberg-Osgood
- S-N curve analysis including multiaxial fatigue using axial stress or a new Brown-Miller analysis formulated for use with S-N curves Wöhler, Basquin
- Dang Van multiaxial fatigue for high cycle design cf. Mieses (HCF – elastic; Hooke)
- ( ) Plots of materials data including the effect of temperature, strain rate etc
- ( ) Advanced analysis methods for fatigue of cast irons NO
- ( ) Analysis of welded joints NO
- ( ) High temperature fatigue included as standard Material data included
- Analysis from elastic and elastic-plastic FEA stresses, linear and non-linear analysis HCF, LCF
- ( ) Automatic detection of surfaces
- Automatic detection of fatigue hotspots, based on user-defined criteria : notches
- ( ) Comprehensive element/node group management
- Stress gradient corrections notches
- ( ) Interfaces to ABAQUS (.fil & .odb), ANSYS (.rst), MSC.Nastran (.op2 & .f06), NX Nastran (.op2 & .f06), NEiNastran (.op02 & .f06), Pro/Mechanica (ASCII & binary), I-deas (.unv), ADAMS, .dac, MTS RPCIII (.rsp), BEASY, FEMSYS, CADFIX, Altair HyperMesh & Optistruct

Ch.7 Ch 8

CRITICAL PLANE MULTIAXIAL STRESS-LIFE & STRAIN-LIFE METHODS ARE INCLUDED AS STANDARD

In materials part

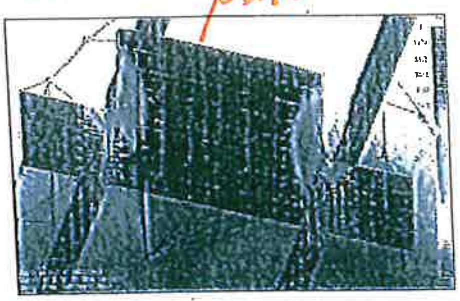

fe-safe™ fatigue contour plot of the internal structure of a transportation container

" fe-safe™ accurately identified the fatigue hotspot critical for the welded section. This allowed the design to be improved early in the design process, thereby avoiding costly redesign downstream"

Portsmouth Aviation, UK

"fe-safe™ – invaluable and indispensable for predictive fatigue analysis"

Eaton Corporation, Automotive Group, USA